Supplementary information

An engineered ClyA nanopore detects folded target proteins by selective external association and pore entry

Misha Soskine[a], Annemie Biesemans[a], Benjamien Moeyaert[a], Stephen Cheley[b], Hagan Bayley[c] and Giovanni Maglia[a1]

[a]*Department of Chemistry, University of Leuven, Leuven, 3001, Belgium*

[b]*Department of Pharmacology, University of Alberta, Edmonton, T6G 2E1, AB Canada*

[c]*Department of Chemistry, University of Oxford, Oxford, OX1 3TA, UK*

Materials and Methods

Materials were purchased from Sigma, unless otherwise specified. DNA was purchased from Integrated DNA Technologies (IDT), enzymes from Fermentas and lipids from Avanti Polar Lipids. The concentrations of the thrombins and hirudin were obtained from their unit concentrations, assuming that 1 NIH unit/mL = 10 nM.[1]

Plasmid preparation

The synthetic gene for ClyA from *Salmonella typhi* was constructed by GenScript. The wild-type gene was modified by the substitution of the two Cys residues (positions 87 and 285) with Ser and by the attachment of DNA encoding a Gly-Ser-Ser linker followed by a C-terminal hexahistidine tag. This construct is referred to as ClyA throughout the paper. The ClyA gene was cloned into a pT7 expression plasmid (pT7-SC1[2]) by using the Nde I (5') and Hind III (3') restriction sites. The S110C-ClyA mutant for the attachment of DNA aptamers was constructed by the PCR-like amplification of the circular plasmid template containing the ClyA gene with Phire® Hot Start DNA Polymerase (Finnzymes) by using two complementary primers. The primers contained a codon encoding the mutation (marked in bold), flanked by sequences complementary to the template: forward – 5'-GAATACAACGAGAAAAAAGCG**TGC**GCGCAGAAAGACATTC and reverse – 5'-GAATGTCTTTCTGCGC**GCA**CGCTTTTTTCTCGTTGTATTC. The PCR product was incubated with Dpn I for 1 h at 37ºC to digest the plasmid template, followed by electroporation into E. cloni® 10G cells (Lucigen). Transformants containing the plasmid were grown overnight at 37ºC on LB agar plates supplemented with 100 mg/L ampicillin. Single colonies were picked and inoculated into 10 mL LB medium

supplemented with 100 mg/L of ampicillin for plasmid DNA preparation. The presence of the mutation was confirmed by sequencing of the plasmid.

Expression and purification of ClyA and the formation of dodecamers

E. coli BL21(DE3)pLysS cells were transformed with the pT7-ClyA plasmid. Transformants were grown overnight at 37ºC on LB agar plates supplemented with 100 mg/L ampicillin. The resulting colonies were inoculated into 500 mL LB medium containing 100 mg/L of ampicillin. The culture was grown at 37ºC, with shaking at 200 rpm, until it reached an OD_{600} of 0.6 to 0.8. The expression of ClyA was then induced by the addition of 0.5 mM IPTG and growth was continued at 20ºC. The next day the bacteria were harvested by centrifugation at 6000 x g for 10 min and the pellets were stored at -70ºC.

The pellets containing monomeric ClyA were thawed and resuspended in 10 to 20 mL of wash buffer (10 mM imidazole, 150 mM NaCl, 15 mM Tris.HCl, pH 7.5), supplemented with 1 mM $MgCl_2$ and 0.05 units/mL of DNAseI (Fermentas). For S110C-ClyA, 15 mM β-mercaptoethanol was included throughout the purification (see below). The bacteria were lysed by the addition of 10 µg/mL of lysozyme and 0.3% w/v SDS, followed by vortexing and incubation at 37ºC for 20 min. The crude lysate was clarified by centrifugation at 6000 x g for 15 min and the supernatant was mixed with 2 mL of Ni-NTA resin (Qiagen) pre-equilibrated with wash buffer. After 1 h, the resin was loaded into a column and washed with 20 column volumes of the wash buffer containing 0.1 % w/v SDS. ClyA was eluted with approximately two column volumes of wash buffer containing 300 mM imidazole and 0.1% SDS (w/v).

Further purification of ClyA monomers was carried out by blue native gel electrophoresis by using a 4-15% polyacrylamide gradient gel (Bio-Rad). To obtain oligomeric ClyA, the band corresponding to the ClyA monomer was excised from the gel (Fig. S4B) and homogenized in gel extraction buffer: 0.2% β-dodecyl maltoside (DDM, GLYCON Biochemicals GmbH), 150 mM NaCl 15 mM Tris.HCl, pH 7.5. Gel debris were sedimented by centrifugation at 20,000 x g for 15 min and the extracted protein was purified once again by blue native gel electrophoresis (see above). The major band of oligomeric ClyA was extracted and stored at 4ºC. For long-term storage, glycerol was added to 15% (v/v) and the protein was flash frozen and stored at -70ºC.

Aptamer conjugation

Lyophilized TBA, 5'-AGTCCGTGGTAGGGCAGGTTGGGGTGACTTTTTTTTT-3',[3] containing a protected thiol group attached to the 3' hydroxyl end of the DNA via a C3 linker (3ThioMC3-D, IDT), and LBA, 5'TTTTTTTTTATCTACGAATTCATCAGGGCTAAAGAGTGCAGAGTTACTTAG-3',[4] containing a protected thiol group attached to the 5' hydroxyl end of the DNA via a C6 linker (5ThioMC6-D, IDT) were dissolved in TAE buffer (40 mM Tris.HCl, 20 mM acetic acid, 1 mM EDTA, pH 8.5), and reduced with 10 mM DTT for 1 h at room temperature.[5] Excess DTT was removed by extraction with ethyl acetate as follows. One volume of ethyl acetate was added to the reduced aptamer solution, which was then vortexed for 5 s. The phases were separated by centrifugation at 20,000 x g for 30 s and the organic phase was removed. The procedure was repeated 5 times, after which the thiolated aptamers in the aqueous phase were reacted with 10 mM 4,4'-dithiopyridine for 1 h at

RT. Excess 4,4'-dithiopyridine was then removed by 5 extractions with diethyl ether. The activated thiolated aptamers were stored frozen at -20ºC.

During the purification of S110C-ClyA monomers, 15 mM β-mercaptoethanol, was included until the final step in which the protein on Ni-NTA resin was washed with 17 column volumes of buffer containing β-mercaptoethanol and then three volumes of thiol-free buffer. Immediately after elution from the Ni-NTA resin, the S110C-ClyA monomer was mixed with 200 μM activated thiolated aptamer and the reaction was allowed to proceed for 2 h at room temperature. ClyA monomers conjugated with aptamers were separated from unmodified monomers by blue native polyacrylamide gel electrophoresis containing 0.1 % SDS (w/v) in the loading buffer. Typically, between 20 to 60% of the S110C-ClyA monomer was conjugated to the aptamer (Fig. S4B). 10 mM EDTA was added to the gel extraction buffer to protect the conjugated aptamers from nuclease degradation.

Expression and purification of FP

Dendra2_M159A was expressed from a pRSETb vector. The construct was transformed into E. coli JM109(DE3) cells (Promega, Madison, Wisconsin, USA). A single transformant was inoculated into 5 mL of LB medium supplemented with ampicillin (100 mg/L) and incubated at 37ºC for 5 h. This starter culture was then transferred to 250 mL of LB medium with ampicillin (100 mg/L) and incubated at 22ºC overnight. The next morning, IPTG was added to 100 μM and the culture was further incubated at 22ºC for 24 h.

Cells from the visibly green culture were harvested by centrifugation at 5000 x g for 10 min. The pellet was resuspended in PBS buffer (50 mL) supplemented with protease inhibitors (cOmplete mini, Roche). The cells were lysed with a French press and the lysate was centrifuged at 10,000 x g for 30 min. The cleared lysate was mixed with 2.5 mL of Ni-NTA agarose (Qiagen), loaded into a gravity-flow column (Pierce) and washed with 10 mL of TN buffer (100 mM Tris.HCl, 300 mM NaCl, pH 7.4, supplemented with 5 mM imidazole). The protein was then eluted with TN buffer containing 300 mM imidazole. The buffer was exchanged for TN buffer without imidazole by using a Vivaspin 15 10'000 MWCO spin column (Sartorius Stedim). The protein concentration was calculated from the absorption spectrum (Shimadzu UV-1650PC) and the extinction coefficient at 471 nm of 51'100 $M^{-1}cm^{-1}$.[6]

Electrical recordings in planar lipid bilayers.

The applied potential refers to the potential of the trans electrode. ClyA nanopores were inserted into lipid bilayers from the cis compartment, which was connected to the ground. The two compartments were separated by a 25-μm thick polytetrafluoroethylene film (Goodfellow Cambridge Limited) containing an orifice ~100 μm in diameter. The aperture was pretreated with ~10 μL of 10% hexadecane in pentane and a bilayer was formed by the addition of ~10 μL of 1,2-diphytanoyl-*sn*-glycero-3-phosphocholine (DPhPC) in pentane (10 mg/mL). Typically, the addition of 0.01-0.1 ng of oligomeric ClyA to the cis compartment (0.5 mL) was sufficient to obtain a single channel. Electrical recordings were carried out in 150 mM NaCl, 15 mM Tris.HCl, except in Figures S3, S5A and S5C where the solution was 75 mM NaCl, 7.5 mM Tris.HCl, pH 7.5. The temperature of the recording chamber was maintained at

28°C by water circulating through a metal case in direct contact with the bottom and sides of the chamber. The data in Figure S5 were collected at room temperature (22 to 23 °C). To cleave the aptamers from a ClyA nanopore, 20 mM DTT (from a freshly prepared 1 M stock) was added to the cis chamber.

Data recording and analysis

Electrical signals from planar bilayer recordings were amplified by using an Axopatch 200B patch clamp amplifier (Axon Instruments) and digitized with a Digidata 1320 A/D converter (Axon Instruments). Data were recorded by using Clampex 10.2 software (Molecular Devices) and the subsequent analysis was carried out with Clampfit software (Molecular Devices). Lysozyme blockades were recorded by applying a 10 kHz low-pass Bessel filter and sampling at 50 kHz. HT, BT and FP blockades were recorded by using a 2 kHz low-pass Bessel filter, with sampling at 10 kHz. Open pore current values (I_O) for ClyA and blocked pore current values (I_B) for HT and BT and their complexes were calculated from Gaussian fits to all points histograms (0.3 pA bin size). Histograms for HT and BT blockades were prepared from at least 10 current blockades typically 0.5 s long. The residual current values (I_{RES}) were calculated as: $I_{RES} = I_B / I_O$ %. When there were two blockade levels, their relative contributions (Fig. 2C) were deduced from the area of the peaks obtained from Gaussian fits to the all points histogram (Fig. S2). I_B values for FP were calculated by applying the “single-channel search” option in the Clampfit software. At least 100 events were recorded for each channel that was analyzed. The duration of the FP blockades (dwell times), which occasionally showed both level 1 and level 2 currents, were distributed over two orders of magnitude and were not fit well with exponential functions. Therefore, median dwell

times are quoted for FP and lysozyme. For the data in Figure S5A, level 1 was set to ~80% of the open pore conductance value, which was described by level 0. Events shorter than 0.5 ms were ignored. The frequency of occurrence of blocking events was calculated by fitting the cumulative distribution of the inter-event intervals for at least 100 events to a single exponential. Graphs were made with Origin (OriginLab Corporation). All values quoted in this work are based on the average of at least three separate recordings, unless otherwise specified. Errors are given as standard deviations.

Additional discussion

Aptamer-ClyA pores and their interactions with analytes

Aptamer-conjugated pores (TBA-ClyA and LBA-ClyA) showed slightly higher open pore conductance values than “naked” ClyA pores (Fig. 4C-D and S4C). The addition of 20 mM DTT, which cleaves the disulfide bonds between the aptamers and the pore (Fig. S6) restored the conductance values to that of the undecorated ClyA pore. Therefore, the presence of DNA at the mouth of the ClyA nanopore increases the conductance of the pore. Although this might appear counterintuitive, it has been observed previously that in 150 mM salt the passage of dsDNA through nanopores in silicon nitride results in an increase in ionic current rather than a block,[7] because at low ionic strength the ionic current that flows during DNA translocation is dominated by the counterions that accumulate around the DNA backbone.[7] Therefore, the increased conductance of aptamer-ClyA nanopores is most likely due to the accumulation of counter ions at the pore mouth.

The capture of protein analytes by ClyA pores was enhanced by the presence of aptamers conjugated atop the pore. We could not investigate this effect in detail, because the binding of proteins to the aptamers did not affect the ionic current. However, we have depicted the aptamers as lying outside the lumen of the pore in the TBA-ClyA nanopore (Fig. 4B), because at negative applied potentials, aptamers attached to the cis surface would have to move against the field to enter the pore. In addition, at -35 mV, the addition of HT to TBA-ClyA pores elicited current blockades (I_{RES} = 54.3 ± 0.7 % and 21.8 ± 0.6 %, for levels 1 and 2 respectively) very similar to the blockades observed with unmodified pores (I_{RES} of 56.0 ± 0.7 % and 23.2 ± 0.7 % for levels 1 and 2 respectively), supporting the notion that the aptamers lie mostly outside the ClyA lumen. It is likely that the increased rate of capture of protein analytes by the aptamer-pore conjugates is due to the increased local concentration of the analyte on top of the nanopore, brought about by transient binding of analytes to the aptamers.

To our surprise, we found that LBA-ClyA and TBA-ClyA nanopores also manifested enhanced capture of the non-cognate analytes HT and lysozyme, respectively. Assuming that the 12 aptamers fit within a cylinder described by the diameter of the pore (7 nm) and the height of the aptamers (2.5 nm), the aptamer concentration at the top of the nanopore is about 0.2 M. Thrombin has two electropositive surfaces, the fibrinogen-recognition and heparin-binding exosites, and displays micro-molar affinity towards non-specific ssDNA molecules.[3] Similarly, lysozyme (pI = 11.4) has an extended electropositive surface (Fig. 1A), and shows sub-micromolar affinity for ssDNA with random sequences.[8] Therefore, it is likely that HT and lysozyme are concentrated at the mouth of ClyA by electrostatic interactions

between the proteins and the DNA. Interestingly, this recognition mechanism is related to that employed by the NPC, where the FG repeat regions bind the molecules to be transported through the pore in low affinity interactions, which are in this case hydrophobic in nature.[9-11]

Finally, we found that the analyte capture frequency for TBA-ClyA pores showed larger variations, as indicated by the error bars (Fig. S5B), compared to “naked” ClyA pores. A possible reason is that relatively few events were collected (typically 100), because thrombin blocks are rare at the low concentration tested (0.1 s^{-1} at 1 nM HT). When thousands of events can be collected (e.g. for lysozyme capture by LBA-ClyA pores), the error bars are smaller (Fig. S5A). In addition, analyte capture rates could show pore-to-pore variation due to the incorporation of unmodified monomers into the ClyA pores (i.e. <12 aptamers per pore), or to aptamer degradation during storage (e.g. by contamination with nucleases). Occasionally, individual TBA-ClyA and LBA-ClyA pores switched between states with different analyte capture efficiencies (10 to 20% variation) on a timescale of few tens of seconds. This might be a consequence of aptamer crowding on top of the pores, which could provoke slow interconversion between states showing different affinities for the analyte.

Additional Figures

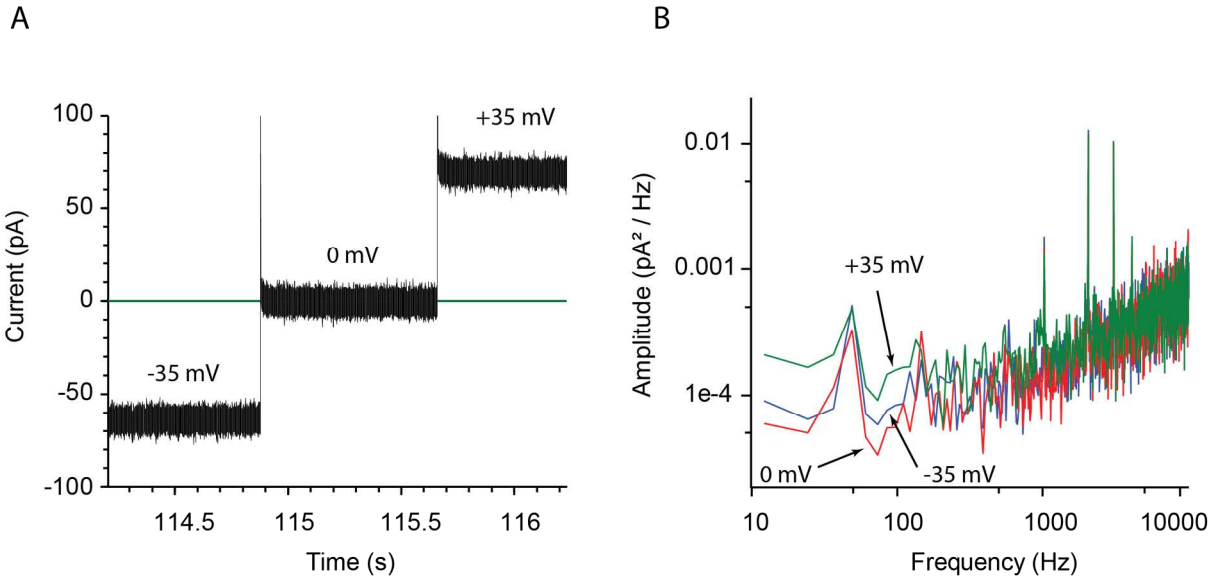

Fig. S1. Noise characteristics of ClyA nanopores in 150 mM NaCl, 15 mM Tris.HCl, pH 7.5. A: Current recording for a single ClyA nanopore at -35 mV (left), 0 mV (center) and +35 mV (right). **B**: Current power spectral densities of the ClyA nanopore used in A at -35 mV (blue), 0 mV (red) and +35 mV (green) obtained from 0.5 s traces. The measurements were performed at a sampling rate of 50 kHz with an internal low-pass Bessel filter set at 10 kHz.

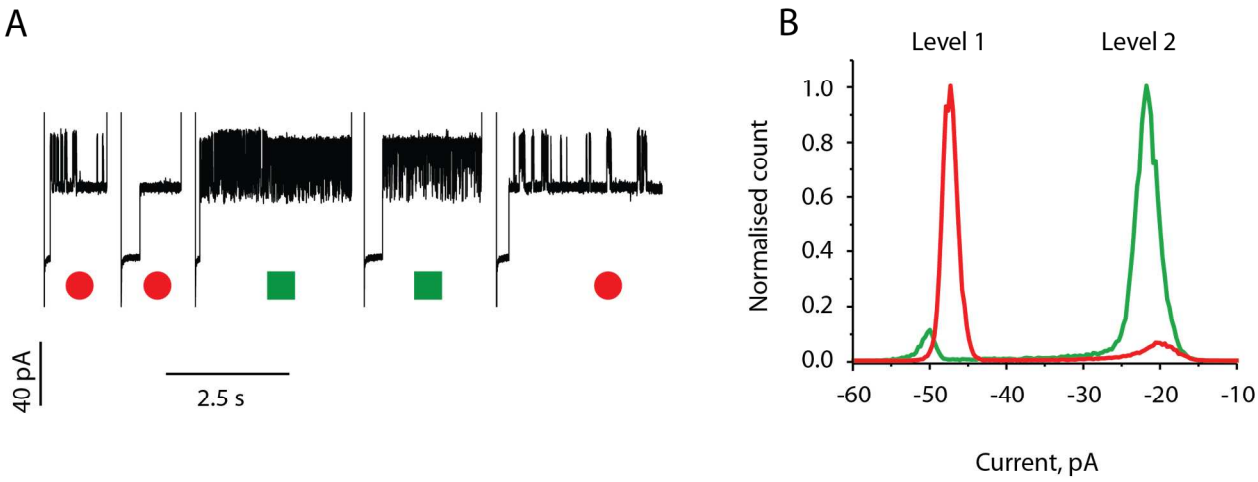

Fig. S2. Thrombin blockades at -50 mV. A: Five consecutive blockades provoked by a mixture of 12 nM HT and 12 nM BT at -50 mV show that blockades elicited by HT (green square) and BT (red spheres) can be easily discriminated. After a thrombin block, the open pore current was restored by manually switching the potential to +35 mV and then back to -35 mV. **B**: All-points histograms calculated from ten HT (green) and ten BT (red) blockades at -50 mV. The data were collected in 150 mM NaCl, 15 mM Tris.HCl, pH 7.5, at 28°C.

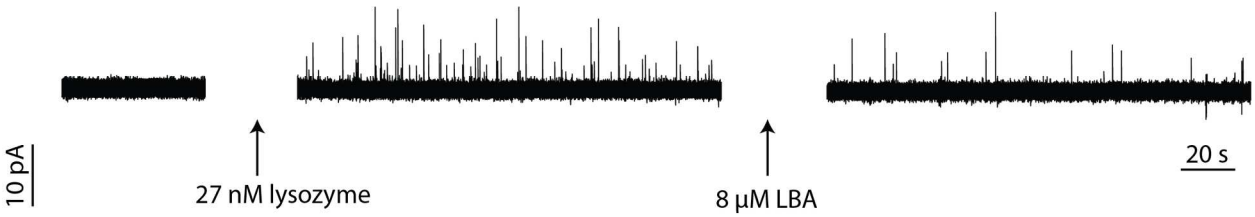

Fig. S3. LBA binding to lysozyme as detected by ClyA pores. Left**,** the addition of 27 nM lysozyme elicits characteristic current blockades. Right, the subsequent addition of 8 µM LBA reduced the frequency of the blockades induced by lysozyme. The data were collected in 70 mM NaCl, 15 mM Tris.HCl, pH 7.5, at 28°C.

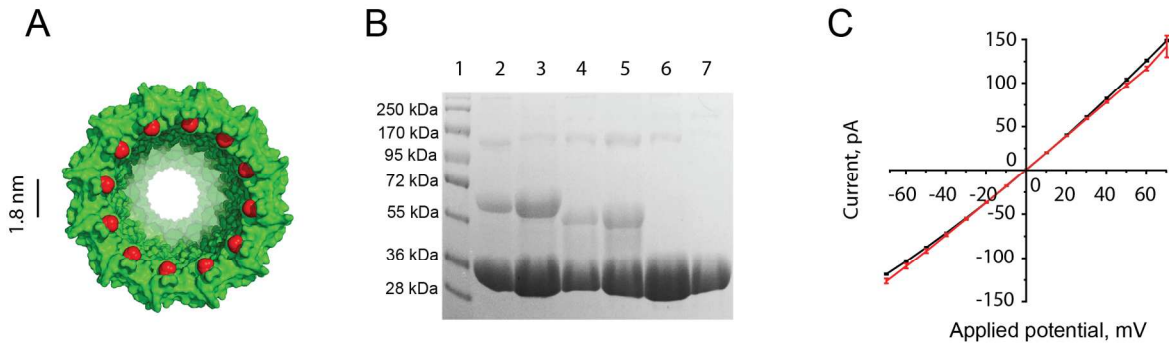

Fig. S4. Preparation and characterization of LBA- and TBA-conjugated ClyA pores. A: Top view of ClyA nanopore (surface representation, Pymol) showing the residues at position 110 (red spheres) to which aptamers are conjugated. The distance between two Cα atoms of neighboring residues 110 is 1.8 nm. **B**: Aptamer attachment to S110C-ClyA monomers examined by electrophoresis in a denaturing, non-reducing 12% SDS-polyacrylamide gel. Lane 1, Markers; lanes 2 and 3 S110C-ClyA monomers after incubation (2 h) with 200 μM of activated thiolated LBA aptamers; lanes 4 and 5, S110C-ClyA monomers after incubation (2 h) with 200 μM of activated thiolated TBA aptamers; lanes 6 and 7, unmodified ClyA monomers. **C**: Current-voltage curves for TBA-ClyA pores (red) and unmodified ClyA pores (black) in 150 mM NaCl, 15 mM Tris.HCl, pH 7.5, at 28°C

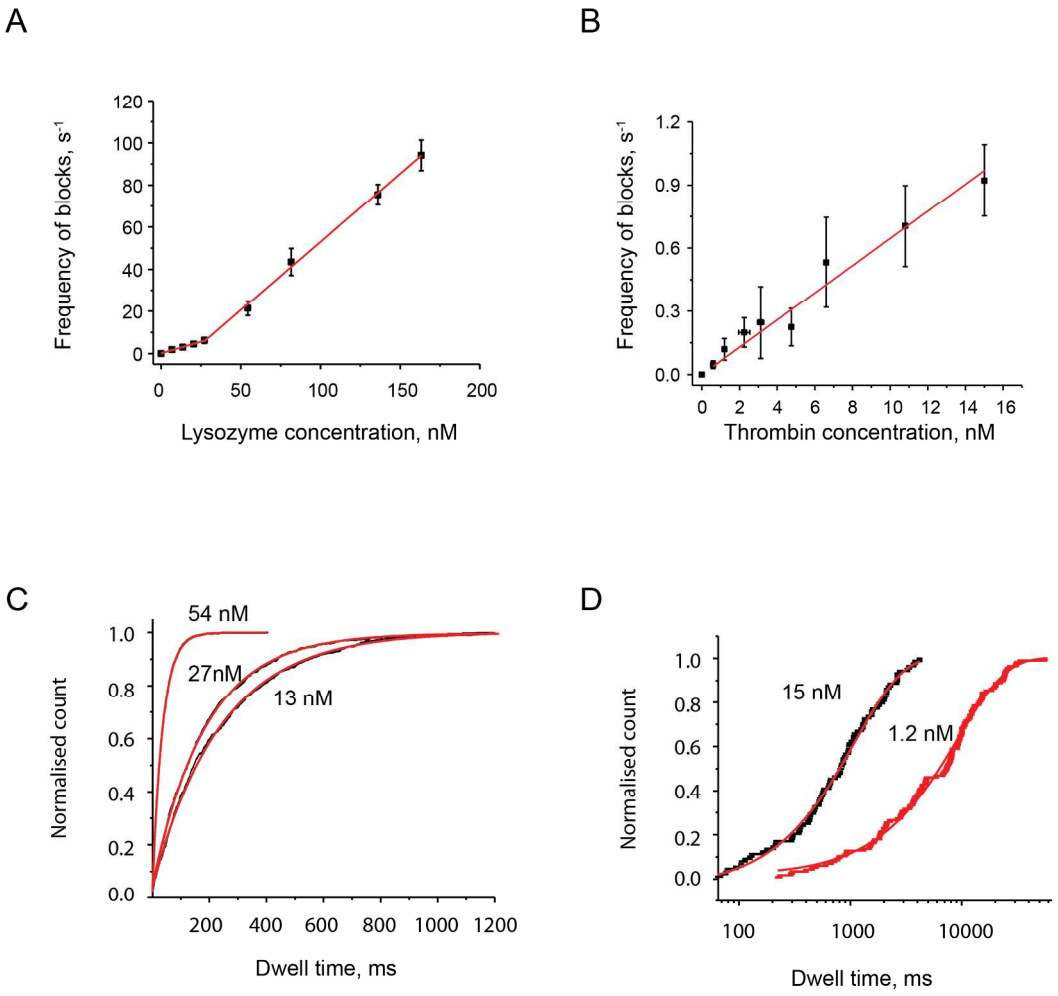

Fig. S5. Dose response for LBA-ClyA and TBA-ClyA. **A, B**: Dependence of the frequency of current blockades on the cognate substrate concentration for LBA-ClyA and TBA-ClyA nanopores, respectively. The red lines indicate linear fits. LBA-ClyA captured lysozyme with different efficiencies depending on the analyte concentration. At concentrations lower than 25 nM, the slope of the linear regression was 222 ± 9 s^{-1} μM^{-1}, while at concentrations higher than 25 nM the slope was 648 ± 17 s^{-1} μM^{-1}. The linear regression slope for thrombin was 65 ± 3 s^{-1} μM^{-1}. Graphical representations of the concentration dependence of ligands binding to receptors, such as Scatchard or Lineweaver–Burk plots, often show a biphasic behavior, which is explained in terms of

multiple binding sites or receptor cooperativity.[12] The two rates measured for lysozyme capture could then reflect a sophisticated relation between the analytes binding to and diffusion through the aptamer forest atop of the nanopore. Nonetheless, this effect could also be due to analyte loss at low proteins concentration due to the partition of lysozyme into the lipid bilayers[13-17] or to adsorption to the chamber walls. The errors are shown as standard deviations except for the slope, where the error is the standard error. **C, D**: Examples of cumulative distributions of the unoccupied pore dwell-times used to determine the lifetime of the unoccupied state (τ_{on} or inter-event interval) for lysozyme (C) and thrombin (D). The red lines indicate the exponential fits used to determine τ_{on}. D is displayed on a logarithmic scale. The data were collected at 22 to 23ºC in 75 mM NaCl, 7.5 mM Tris.HCl, pH 7.5, at -10 mV (A and C) and in 150 mM NaCl, 15 mM Tris.HCl, pH 7.5, at -35 mV (B and D).

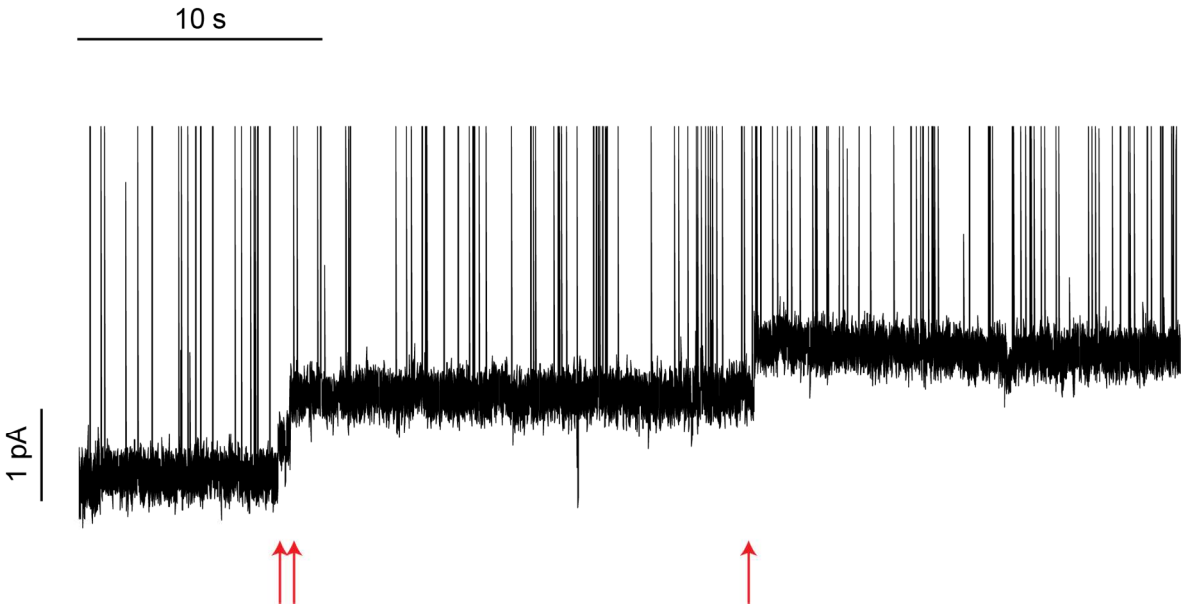

Fig. S6. Cleavage of aptamers from TBA-ClyA pores: Upon the addition of 20 mM DTT to TBA-ClyA pores, the ionic current decreased by steps of 0.45 ± 0.06 pA (red arrows), indicating that the disulfide bonds connecting individual aptamers to ClyA are reduced and the aptamers cleaved off the pore. After 10 min, 11 cleavage events could be assigned from this trace. Vertical current lines indicate the binding of FP (268 nM) to ClyA (Fig. 4D). An additional 200 Hz Bessel filter was digitally applied to the current trace after recording. The data were collected in 150 mM NaCl, 15 mM Tris.HCl, pH 7.5, at 28°C.

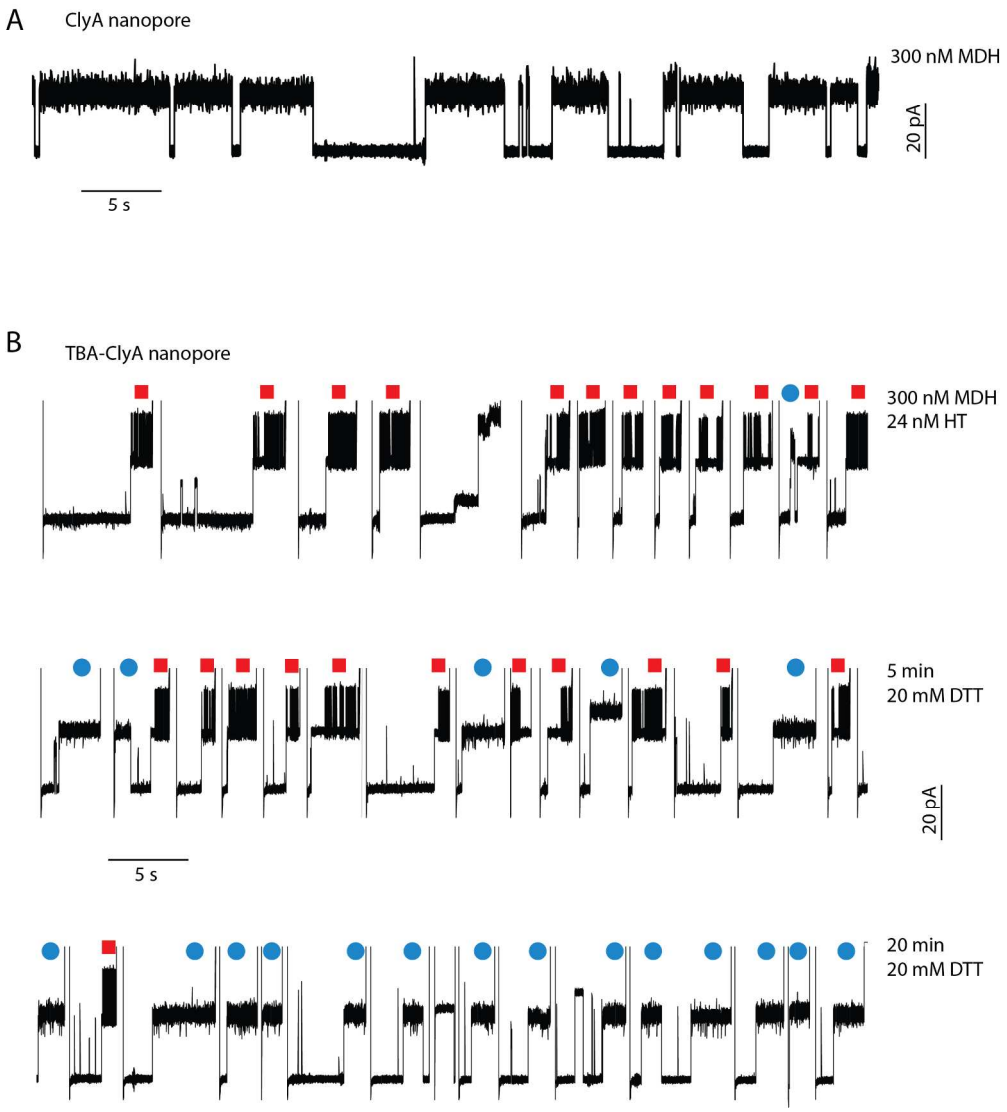

Fig. S7 Selective detection by TBA-ClyA pores in the presence of malate dehydrogenase. A, Blocks to the ClyA open pore current provoked by 300 nM dimeric malate dehydrogenase from pig heart (MDH, monomer of 35 kDa). **B,** Selective sensing with TBA-ClyA pores**.** Top, a single TBA-ClyA pore in the presence of 300 nM MDH and 24 nM HT. 90 ± 4% of the current blockades observed are assigned as HT blocks (red squares, n = 3). Middle: 5 min after the addition of 20 mM DTT. Current blockades assigned to MDH (blue circles) become more frequent, suggesting that some of the aptamers have been cleaved off the top of the pore. Bottom, 20 min after the addition of

20 mM DTT. 91 ± 1% of the blockades are assigned as MDH blocks (n = 3). The traces were recorded at -35 mV in 150 mM NaCl, 15 mM Tris.HCl, pH 7.5, at 28°C.

REFERENCES

1) Kunapuli, S. P. *et al.* Thrombin-induced platelet aggregation is inhibited by the heptapeptide Leu271-Ala277 of domain 3 in the heavy chain of high molecular weight kininogen. *J Biol Chem* 271, 11228-11235 (1996).
2) Miles, G., Cheley, S., Braha, O. & Bayley, H. The staphylococcal leukocidin bicomponent toxin forms large ionic channels. *Biochemistry* 40, 8514-8522, doi:bi010454o [pii] (2001).
3) Tasset, D. M., Kubik, M. F. & Steiner, W. Oligonucleotide inhibitors of human thrombin that bind distinct epitopes. *J Mol Biol* 272, 688-698, doi:S0022-2836(97)91275-4 [pii]

10.1006/jmbi.1997.1275 (1997).
4) Kirby, R. *et al.* Aptamer-based sensor arrays for the detection and quantitation of proteins. *Anal Chem* 76, 4066-4075, doi:10.1021/ac049858n (2004).
5) Rotem, D., Jayasinghe, L., Salichou, M. & Bayley, H. Protein detection by nanopores equipped with aptamers. *J Am Chem Soc* 134, 2781-2787, doi:10.1021/ja2105653 (2012).
6) Adam, V. *et al.* Rational design of photoconvertible and biphotochromic fluorescent proteins for advanced microscopy applications. *Chem Biol* 18, 1241-1251, doi:S1074-5521(11)00315-2 [pii]

10.1016/j.chembiol.2011.08.007 (2011).
7) Smeets, R. M. M. *et al.* Salt dependence of ion transport and DNA translocation through solid-state nanopores. *Nano Letters* 6, 89-95, doi:Doi 10.1021/Nl052107w (2006).
8) Potty, A. S., Kourentzi, K., Fang, H., Schuck, P. & Willson, R. C. Biophysical characterization of DNA and RNA aptamer interactions with hen egg lysozyme. *Int J Biol Macromol* 48, 392-397, doi:S0141-8130(10)00368-5 [pii]

10.1016/j.ijbiomac.2010.12.007 (2011).
9) Aitchison, J. D. & Rout, M. P. The Yeast Nuclear Pore Complex and Transport Through It. *Genetics* 190, 855-883 (2012).
10) Bednenko, J., Cingolani, G. & Gerace, L. Importin beta contains a COOH-terminal nucleoporin binding region important for nuclear transport. *J Cell Biol* 162, 391-401, doi:10.1083/jcb.200303085

jcb.200303085 [pii] (2003).
11) Bayliss, R., Littlewood, T., Strawn, L. A., Wente, S. R. & Stewart, M. GLFG and FxFG nucleoporins bind to overlapping sites on importin-beta. *J Biol Chem* 277, 50597-50606, doi:10.1074/jbc.M209037200

M209037200 [pii] (2002).
12) Wilson, K. & Walker, J. *Principles and Techniques of Biochemistry and Molecular Biology*. (Cambridge University Press, 2010).
13) Nodake, Y., Iwasaki, K. & Yamasaki, N. Interactions of a lysozyme-monomethoxypolyethylene glycol conjugate with lipopolysaccharides and lipid bilayers and effects of conjugate on gram-negative bacteria. *Biosci Biotechnol Biochem* 66, 1848-1852 (2002).

14) Witoonsaridsilp, W., Panyarachun, B., Sarisuta, N. & Muller-Goymann, C. C. Influence of microenvironment and liposomal formulation on secondary structure and bilayer interaction of lysozyme. *Colloids Surf B Biointerfaces* 75, 501-509, doi:S0927-7765(09)00460-3 [pii]

10.1016/j.colsurfb.2009.09.027 (2010).
15) Zlatanov, I. & Popova, A. Penetration of lysozyme and cytochrome C in lipid bilayer: fluorescent study. *J Membr Biol* 242, 95-103, doi:10.1007/s00232-011-9380-8 (2011).
16) Al Kayal, T. *et al.* Lysozyme interaction with negatively charged lipid bilayers: protein aggregation and membrane fusion. *Soft Matter* 8, 4524-4534 (2012).
17) Kim, J. & Kim, H. Penetration and fusion of phospholipid vesicles by lysozyme. *Arch Biochem Biophys* 274, 100-108, doi:0003-9861(89)90420-7 [pii] (1989).